Nonlinear AC magnetic susceptibility of the stage-2 $CoCl_2$ graphite intercalation compound

2002 J. Phys.: Condens. Matter 14 5583

(http://iopscience.iop.org/0953-8984/14/22/311)

INSTITUTE OF PHYSICS PUBLISHING JOURNAL OF PHYSICS: CONDENSED MATTER

J. Phys.: Condens. Matter **14** (2002) 5583–5599 PII: S0953-8984(02)33483-0

Nonlinear AC magnetic susceptibility of the stage-2 $CoCl_2$ graphite intercalation compound

Masatsugu Suzuki, Itsuko S Suzuki and Ting-Yu Huang

Department of Physics, State University of New York at Binghamton, Binghamton, NY 13902-6016, USA

E-mail: suzuki@binghamton.edu (Masatsugu Suzuki) and itsuko@binghamton.edu (Itsuko S Suzuki)

Received 5 February 2002, in final form 7 March 2002
Published 23 May 2002
Online at stacks.iop.org/JPhysCM/14/5583

Abstract
The stage-2 $CoCl_2$ graphite intercalation compound behaves magnetically like a quasi-two-dimensional XY-like ferromagnet with a very weak antiferromagnetic interplanar exchange interaction. This compound undergoes two magnetic phase transitions at T_{cl} (=6.8–7.2 K) and T_{cu} (=8.9 K). The SQUID AC magnetic susceptibility at a fixed AC frequency ($f = 1$ Hz) has been measured as a function of AC magnetic field strength h (1 mOe $\leqslant h \leqslant$ 4.2 Oe), temperature T ($1.9 \leqslant T \leqslant 12$ K) and external magnetic field ($0 \leqslant H \leqslant 1$ kOe). The dispersion (Θ_1'/h) and absorption (Θ_1''/h) are strongly dependent on h for $h > 50$ mOe in the vicinity of T_{cl} and T_{cu}, where $\Theta_1'/h = \chi_1' + 3\chi_3'h^2/4 + \cdots$ and $\Theta_1''/h = \chi_1'' + 3\chi_3''h^2/4 + \cdots$. We find (i) a shift of T_{cl} in χ_1'' to the low-temperature side with decreasing frequency and (ii) a positive local maximum in χ_3' at 7.3 K. These results are indicative of a re-entrant spin-glass-like phase below T_{cl}, where the AF phase and spin-glass phase coexist. A positive broad peak of χ_3' around 8.4–8.9 K shows the occurrence of two-dimensional ferromagnetic order below T_{cu}. The H–T phase diagram is also determined for H along the c plane.

1. Introduction

Phase transitions of the stage-2 $CoCl_2$ graphite intercalation compound (GIC) have been extensively studied [1,2]. This compound magnetically behaves like a quasi-two-dimensional XY-like ferromagnet with a very weak antiferromagnetic (AF) interplanar exchange interaction. It undergoes magnetic phase transitions at T_{cu} (=8.9 K) and T_{cl} (=6.8–7.2 K). The intercalate layers are formed of small islands whose diameters are of the order of 450 Å. The existence of such islands is essential to the successive phase transitions. The nearest-neighbour spins inside islands are ferromagnetically coupled with intraplanar exchange interactions. On approaching T_{cu} from the high-temperature (T) side, spins come to order ferromagnetically inside islands. At T_{cu} these ferromagnetic (FM) islands continue to order over the same layer through interisland interactions (mainly FM), forming a two-dimensional FM long-range order with Ising symmetry. The spin easy axis is a reference axis in the c plane perpendicular to the c axis, which may coincide with the direction of the in-plane anisotropic field (see 2.2). It is believed that below T_{cl} a three-dimensional-like AF long-range order is established through effective AF interplanar interactions between spins in adjacent intercalate layers. The critical behaviour below T_{cl} belongs to the universality class of three-dimensional Ising.

However, such an explanation for the ordered phase below T_{cl} may be inconsistent with the following two experimental results.

(i) In our previous paper [3] we studied the temperature (T) and frequency (f) dependence of the absorption (Θ_1''/h) using SQUID AC magnetic susceptibility, where f ($0.1 \leqslant f \leqslant 1000$ Hz) and h (=50 mOe) are the frequency and amplitude of an AC magnetic field, respectively. The absorption Θ_1''/h shows peaks at T_{cl} and T_{cu}. The peak at T_{cl} shifts to the high-T side with increasing f, while the peak at T_{cu} remains unshifted.

(ii) The deviation of the zero-field-cooled (ZFC) susceptibility χ_{ZFC} at an external magnetic field ($H = 1$ Oe) along the c plane (perpendicular to the c axis) from the field-cooled (FC) susceptibility χ_{FC} occurs below 10.7 K, well above T_{cu} [3]. Such an irreversible effect of susceptibility indicates the existence of a spin frustration effect. Thus it is expected that the low-temperature phase below T_{cl} may be a re-entrant spin-glass (RSG) phase, where spin-glass behaviour and AF order coexist. Such a mixed phase is predicted by the mean-field theory of RSG [4].

In this paper we study the phase transitions at T_{cl} and T_{cu} by measuring the linear and nonlinear SQUID AC magnetic susceptibility of the stage-2 $CoCl_2$ GIC. This work allows one to further understand the nature of the possible mixed phase below T_{cl}. In spite of such interest, so far there have been very few studies on the nonlinear AC magnetic susceptibility in the stage-2 $CoCl_2$ GIC [5,6]. We have measured the dispersion Θ_1'/h and absorption Θ_1''/h at fixed temperatures as a function of h, where 1 mOe $\leqslant h \leqslant$ 4.2 Oe and $f = 1$ Hz. Both Θ_1'/h and Θ_1''/h are strongly dependent on h in the vicinity of T_{cl} and T_{cu}, suggesting the existence of nonlinear magnetic susceptibility. We determine the T dependence of nonlinear AC magnetic susceptibilities (χ_3', χ_5', χ_3'' and χ_5'') from the least-squares fits of the data to the power-law forms: $\Theta_1'/h = \chi_1' + 3\chi_3'h^2/4 + \cdots$ and $\Theta_1''/h = \chi_1'' + 3\chi_3''h^2/4 + \cdots$. The T dependence of nonlinear AC magnetic susceptibility χ_3' around T_{cl} and T_{cu} is discussed in comparison with theories (section 2.1).

It is well known that, due to the thermal fluctuations and the increasing short-range order around a spin freezing temperature T_{SG}, pronounced nonlinearities appear in the magnetization of a spin glass (SG). In the presence of H, the DC magnetization M of magnetic systems can be expressed as $M = \chi_1 H + \chi_3 H^3 + \chi_5 H^5 + \cdots$. The nonlinear susceptibility (χ_3, χ_5, $\ldots$) has played a significant role in studying phase transitions of SG systems [4,7]. It is now established that for SG systems χ_3 shows a negative divergence at a spin-freezing temperature T_{SG}, which is regarded as evidence of the cooperative phase transition. For RSG systems, in contrast, there have been only a few studies on χ_3 experimentally and theoretically. The RSG systems undergo successive transitions: one is between the paramagnetic (PM) phase and long-range ordered phase (FM or AF phase) at high temperature and the other is between the ordered phase and the RSG phase at lower temperature. Theoretically Takayama [8] has studied the linear and nonlinear susceptibility of mean-field Ising models for RSG systems by means of Parisi's replica-symmetry-breaking (RSB) scheme (see section 2.1). He has predicted that both FM-based and AF-based RSG systems undergo a transition between the replica-symmetry (RS) phase and the RSB phase at a transition temperature T_{RSG}, keeping spontaneous (staggered) magnetization finite. The nonlinear susceptibility χ_3 exhibits a positive cusp but does not diverge at T_{RSG}. Experimentally χ_3 shows a positive cusplike peak at T_{RSG} for FM-base RSG systems such as (PdFe)Mn [9], $Fe_{3-c}Mn_cS$ [10] and NiMn [11], while χ_3 seems to exhibit a negative divergent singularity at T_{RSG} for AF-base RSG systems such as $Mn_cMg_{1-c}TiO_3$ [12] and $Fe_cMn_{1-c}TiO_3$ [13].

2. Background

2.1. Nonlinear magnetic susceptibility of mean-field Ising model for RSG

The mean-field theory based on the Sherrington–Kirkpatrick (SK) model [14] is the only one that can describe all the SG properties consistently, though qualitatively. The SK model [15] consists of Ising spins with infinite-range random interactions which obey a Gaussian distribution with the mean J_0/N and the variance J_1^2/N, where N is the total number of spins. It is predicted that the system with $J_0 > J_1$ ($H = 0$) exhibits a transition from the PM phase to the FM phase at T_c and a transition from the FM phase to the RSB phase at T_{RSG} ($<T_c$). The RS solution is correct only above T_{RSG}. In the RSB phase below T_{RSG}, there exist many local minima of the free energy (pure states) whose organization is properly described by the Parisi RSB solution. The ordinary FM phase transition occurs at T_c within the RS scheme.

Takayama [8] has calculated explicitly the linear and nonlinear magnetic susceptibility for one of the free-energy local minima (pure state) in the RSB phase, where the system is trapped. They are fast responses as compared with the equilibrium response (slow response), in which reconstruction of global free-energy structure by H is involved. At and below T_{RSG} the spontaneous magnetization M does not vanish (so the RSB phase is called the mixed phase). Spins in a pure state in the RSB phase are frozen more cooperatively than those estimated by the RS solution incorrectly extrapolated to the T range below T_{RSG}. Consequently, the susceptibilities χ_1 and χ_3 exhibit a positive cusp at T_{RSG}. However, they do not diverge at T_{RSG}. This is due to the fact that the mode responsible for the RS instability does not correlate with the uniform magnetization mode. Therefore a cusplike structure in χ_3, instead of divergence, is considered to be one of the crucial tests to check whether the present mean-field picture can be applied or not to transition to the mixed phase. Among quantities which are associated with an individual pure state and can be measured by AC susceptibility, only a spin relaxation time exhibits diverging behaviour at T_{RSG}. The susceptibilities χ_1 and χ_3 decrease quite significantly when the system enters the mixed phase below T_{RSG}.

2.2. Spin Hamiltonian of the stage-2 $CoCl_2$ GIC

The spin Hamiltonian appropriate to Co^{2+} ions (fictitious spin $S = 1/2$) in the stage-2 $CoCl_2$ GIC can be expressed by [16]

$$H = -2J\sum_{\langle i,j\rangle}\boldsymbol{S}_i\cdot\boldsymbol{S}_j + 2J_A\sum_{\langle i,j\rangle}S_i^zS_j^z - 2J'\sum_{\langle i,m\rangle}\boldsymbol{S}_i\cdot\boldsymbol{S}_m - g_a\mu_B SH_A^{in}\sum_i\cos(6\theta_i), \qquad (1)$$

where $\langle i, j\rangle$ denotes nearest-neighbour pairs on the same intercalate layer and $\langle i, m\rangle$ denotes nearest-neighbour pairs on the adjacent intercalate layers, J (=7.75 K) is the FM intraplanar exchange interaction, J_A (=3.72 K) is the anisotropic exchange interaction showing XY anisotropy, J' (<0) is the AF interplanar exchange interaction ($|J'|/J \approx 10^{-4}$), H_A^{in} is the in-plane sixfold-symmetry-breaking field in the c plane and θ_i is the direction of the spin vector $\boldsymbol{S}_i$ with respect to a reference axis. For convenience we define the intraplanar exchange field, interplanar exchange field and XY-like anisotropy field as $H_E = (2zJS/g_a\mu_B)$, $H_E' = (2z'|J'|S/g_a\mu_B)$ and $H_A^{out} = (2zJ_AS/g_c\mu_B)$, respectively. Since z (=6) and z' (=6) are the numbers of intraplanar and interplanar nearest-neighbour Co atoms, and g_a (=6.4) and g_c (=4.75) are the Landé g factors along the a axis (any direction in the c plane) and c axis, respectively, we have $H_E = 108.2$ kOe and $H_A^{out} = 70.0$ kOe. The magnitude of H_E' and H_A^{in} will be discussed in section 5.1.

3. Experimental procedure

The nonlinear magnetic susceptibility can be measured by detecting harmonics of the response to an AC magnetic field (=$h\cos(\omega t)$) at angular frequency ω (= $2\pi f$). The AC magnetization $M(\omega, t)$ induced in the system can be described by a function of odd angular frequency $(2n+1)\omega$ ($n = 0, 1, 2, 3, \ldots$) [17, 18],

$$M(\omega, t) = \sum_{n=0}^{\infty}\{\Theta'_{2n+1}\cos[(2n+1)\omega t] + \Theta''_{2n+1}\sin[(2n+1)\omega t]\}, \tag{2}$$

because of the symmetric hysteresis loop, where

$$\frac{\Theta'_1}{h} = \chi'_1 + \frac{3}{4}\chi'_3 h^2 + \frac{10}{16}\chi'_5 h^4 + \frac{35}{64}\chi'_7 h^6 + \cdots, \tag{3}$$

$$\frac{\Theta'_3}{h^3} = \frac{1}{4}\chi'_3 + \frac{5}{16}\chi'_5 h^2 + \frac{21}{64}\chi'_7 h^4 + \cdots, \tag{4}$$

and similarly for the imaginary part Θ''_{2n+1}. Here χ'_{2n+1} and χ''_{2n+1} are the real and imaginary parts of nonlinear magnetic susceptibility, respectively. Experimentally Θ'_{2n+1} and Θ''_{2n+1} can be determined from the in-phase and out-of phase $(2n+1)\omega$ component in the AC magnetization measurement. In the present work we measured the first harmonic of the AC magnetization, Θ'_1 and Θ''_1 with respect to a response of an AC magnetic field $h\cos(\omega t)$.

The nonlinear magnetic susceptibility of the stage-2 $CoCl_2$ GIC was measured using a SQUID magnetometer (Quantum Design, MPMS XL-5) with AC susceptibility option. Before setting up a sample at 298 K, the remanent magnetic field in the superconducting magnet was reduced to <3 mOe using an ultra-low-field capability option. For convenience, hereafter this remanent field is noted as the state of $H = 0$. The sample was cooled from 298 to 1.9 K at $H = 0$. The measurements were carried out for $H = 0$ at the fixed temperature T. The AC magnetic field ($h\cos(\omega t)$) was applied along a direction (in the c plane) perpendicular to the c axis. The sample used in the present work, which was the same one as used in the previous work [3], is based on single-crystal kish graphite composed of many misoriented crystallites. It had crystal textures with random in-plane orientation and a c-axis mosaic spread (several degrees). The demagnetization effect can be neglected. The amplitude of AC magnetic field was varied from $h = 1$ mOe to 4.2 Oe. The frequency f of the AC magnetic field is 1 Hz. After each h-scan measurement at fixed T, T was increased by $\Delta T = 0.1$ K in the temperature range between 1.9 and 12.0 K. Both Θ'_1/h and Θ''_1/h were measured as a function of h and T.

4. Results

4.1. Linear AC susceptibility

We have measured (i) the T dependence of Θ'_1/h and Θ''_1/h ($h = 50$ mOe and f ($0.01 \leqslant f \leqslant 1000$ Hz)) corresponding to the linear susceptibilities χ'_1 and χ''_1. The experimental procedure for this measurement was the same as used in the previous work [3]. Figure 1 shows the T dependence of Θ''_1/h at various f, where $h = 50$ mOe and h is applied along the c plane. The absorption Θ''_1/h consists of three peaks at T_{cl}, T_p, and T_{cu} ($T_{cl} < T_p < T_{cu}$). The peak

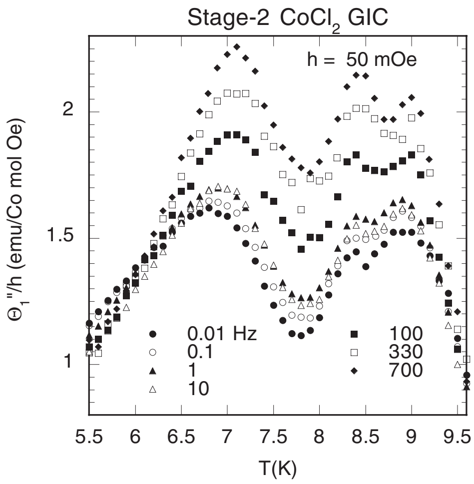

Figure 1. T dependence of Θ_1''/h at various f for the stage-2 $CoCl_2$ GIC: $h = 50$ mOe, $h \perp c$ (c: c axis); $f = 0.01$–1000 Hz.

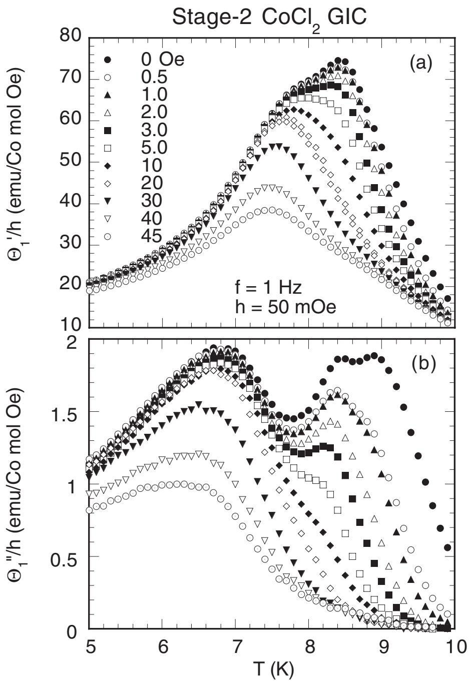

Figure 2. T dependence of (a) Θ_1'/h and (b) Θ_1''/h at various H: $H \perp c$, $h \perp c$, $h = 50$ mOe, $f = 1$ Hz.

temperature T_{cl} increases with increasing f from 6.8 K at 0.01 Hz to 7.2 K at 1 kHz, while T_p and T_{cu} remain unchanged: $T_{cu} = 8.9$ K and $T_p = 8.4$ K. In contrast to the case of Θ_1''/h, the corresponding dispersion Θ_1'/h shows a single peak at T_p, which is independent of f for $0.01 \leqslant f \leqslant 1000$ Hz. The f dependence of T_{cl} will be discussed in section 5.2 in association with the RSG phase.

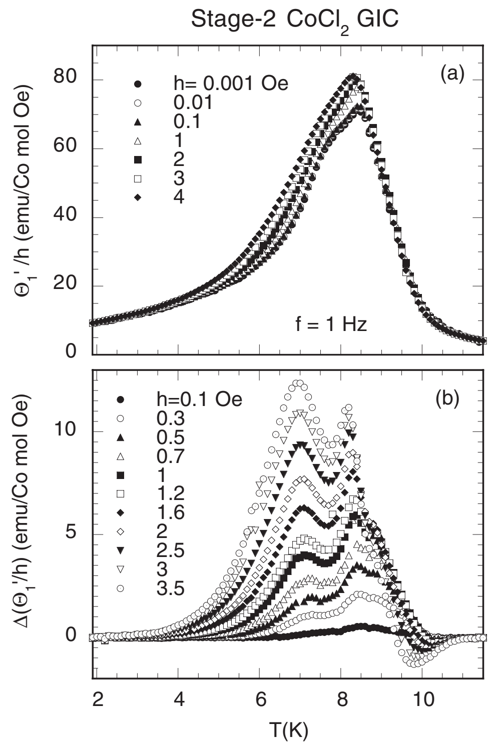

Figure 3. (a) T dependence of Θ_1'/h at various h: $h \perp c$, $f = 1$ Hz, $H = 0$. (b) T dependence of $\Delta(\Theta_1'/h)$ at various h, where $\Delta(\Theta_1'/h)$ is defined by the difference between Θ_1'/h at h ($h > 20$ mOe) and Θ_1'/h at $h = 20$ mOe.

We have also measured the T dependence of Θ_1'/h and Θ_1''/h ($h = 50$ mOe and $f = 1$ Hz) at various H, where H is applied along the c plane perpendicular to the c axis. Figures 2(a) and (b) show the T dependence of Θ_1'/h and Θ_1''/h at various H, where $h = 50$ mOe, and $f = 1$ Hz. The peak of Θ_1''/h at T_{cu} for $H = 0$ disappears at $H = 0.5$ Oe. In contrast, the peaks of Θ_1''/h at T_{cl} and T_p for $H = 0$ change in a complicated manner with H. The peak temperatures of Θ_1'/h and Θ_1''/h are plotted as a function of H, leading to the H–T diagram (see section 5.1 for details).

4.2. Nonlinear AC susceptibility

4.2.1. T dependence of Θ_1'/h *at various h.* Figure 3(a) shows the T dependence of Θ_1'/h at various h, where $f = 1$ Hz. The dispersion Θ_1'/h has an inflection point around 7.2 K and a single peak at T_p (=8.4 K), irrespective of h. The magnitude of Θ_1'/h is dependent on h between 5 and 9 K. We note that the T dependence of Θ_1'/h for $h \leqslant 20$ mOe is independent of h, corresponding to the linear susceptibility χ_1'. Here for convenience we define the nonlinear susceptibility $\Delta(\Theta_1'/h)$ as the difference between Θ_1'/h at h ($h > 20$ mOe) and Θ_1'/h at $h = 20$ mOe. The data of Θ_1'/h at $h = 1$ mOe are not used for the definition of $\Delta(\Theta_1'/h)$ because of relatively large experimental errors. Figure 3(b) shows the T dependence of $\Delta(\Theta_1'/h)$ for stage-2 $CoCl_2$ GIC at various h. The T dependence of $\Delta(\Theta_1'/h)$ is very different from that of Θ_1'/h near T_{cl} and T_{cu} for the same h. For $h = 0.2$ Oe, $\Delta(\Theta_1'/h)$ has a cusp at 7.3 K and a peak at 8.5 K. For $0.5 \leqslant h \leqslant 2$ Oe, $\Delta(\Theta_1'/h)$ has two peaks near T_{cl} and T_p, and a cusp near T_{cu}. The sign of $\Delta(\Theta_1'/h)$ at $h = 0.1$ Oe changes from negative to

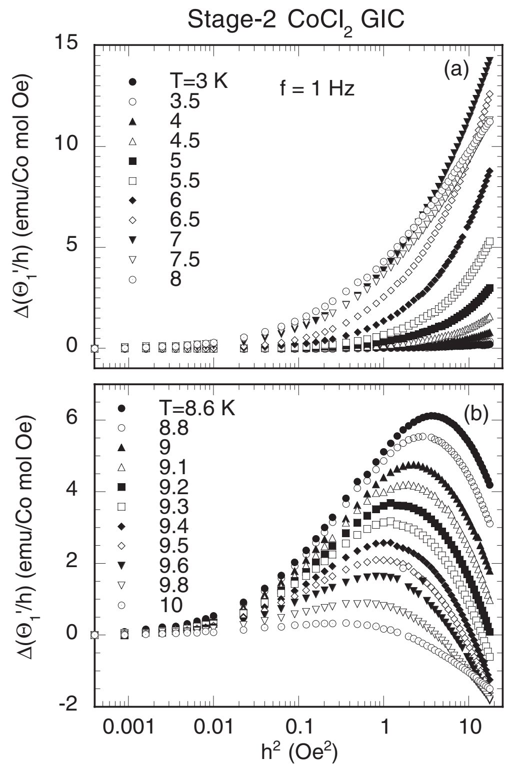

Figure 4. (a) and (b) h^2 dependence of $\Delta(\Theta_1'/h)$ at various T: $f = 1$ Hz.

positive around 10.2 K with decreasing T. The zero-crossing temperature T_x decreases with increasing h: $T_x = 9$ K at $h = 4.2$ Oe. Figures 4(a) and (b) show $\Delta(\Theta_1'/h)$ as a function of h^2 at various T. For $8.3 \leqslant T \leqslant 10.5$ K, $\Delta(\Theta_1'/h)$ shows a peak at a characteristic field h_p. Note that h_p decreases with increasing T: $h_p = 1.5$ Oe at 9.0 K and 0.6 Oe at 10 K. The peak value of $\Delta(\Theta_1'/h)$ at $h = h_p$ drastically decreases with increasing T.

4.2.2. T dependence of Θ_1''/h at various h. Figure 5 shows the T dependence of Θ_1''/h for the stage-2 $CoCl_2$ GIC at various h, where $f = 1$ Hz. Unlike the case of Θ_1'/h, the T dependence of $\Delta(\Theta_1''/h)$ is very similar to that of Θ_1''/h. The absorption Θ_1''/h has three peaks near T_{cl}, T_p and T_{cu}. The heights of these peaks drastically increase with increasing h, reflecting the enhancement of nonlinear susceptibility. Note that the peak around T_{cl} slightly shifts to the high-T side with increasing h for $h \leqslant 1$ Oe and shifts to the low-T side with further increasing h. Figures 6(a) and (b) show $\Delta(\Theta_1''/h)$ as a function of h^2 at various T. Note that the h^2 dependence of $\Delta(\Theta_1''/h)$ is similar to that of $\Delta(\Theta_1'/h)$ for the same T. For $1.9 \leqslant T \leqslant 8.2$ K, $\Delta(\Theta_1''/h)$ increases with increasing h^2. For $8.3 \leqslant T \leqslant 10.8$ K, $\Delta(\Theta_1''/h)$ increases with increasing h^2, showing a peak around h_p, and decreases with further increasing h^2. For $T \geqslant 10.9$ K, $\Delta(\Theta_1''/h)$ decreases with increasing h^2.

4.2.3. Analysis. We analyse the h^2 dependence of $\Delta(\Theta_1'/h)$ and $\Delta(\Theta_1''/h)$ at various T for low h ($h \leqslant 0.5$ Oe). The deviation of $\Delta(\Theta_1'/h)$ and $\Delta(\Theta_1''/h)$ from zero (the so-called nonlinearity) appears even at $h = 0.05$ Oe. For $T > 10.3$ K, $\Delta(\Theta_1'/h)$ decreases with

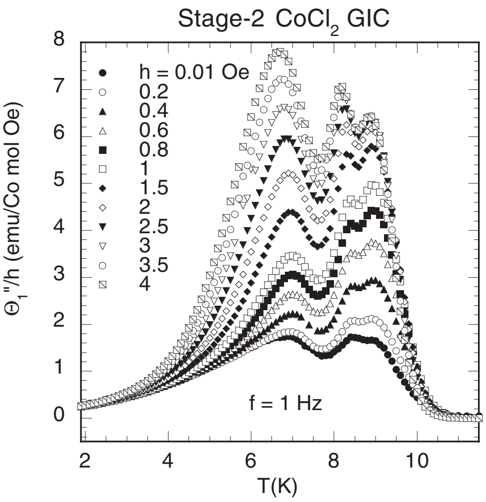

Figure 5. T dependence of Θ_1''/h at various h: $h \perp c$, $f = 1$ Hz, $H = 0$.

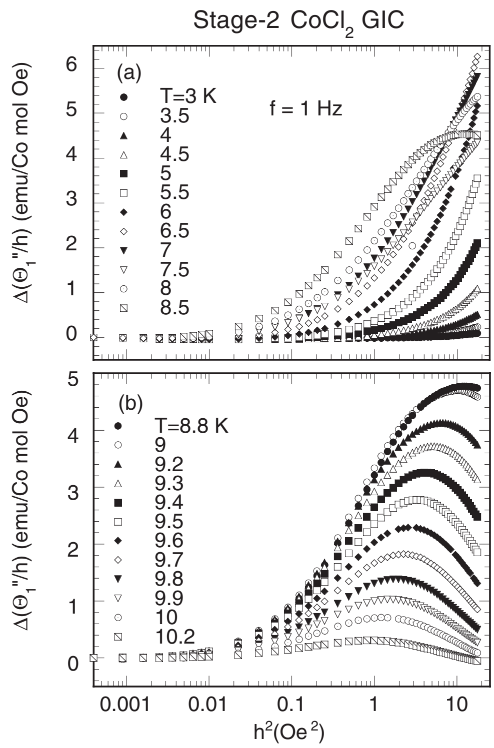

Figure 6. (a) and (b) h^2 dependence of $\Delta(\Theta_1''/h)$ at various T: $f = 1$ Hz, where $\Delta(\Theta_1''/h)$ is defined by the difference between Θ_1''/h at h ($h > 20$ mOe) and Θ_1''/h at $h = 20$ mOe.

increasing h^2 at very low h^2, indicating that χ_3' is negative. For $T < 10.2$ K, $\Delta(\Theta_1'/h)$ increases with increasing h^2 at very low h^2, indicating that χ_3' is positive. The least-squares fit of the data of Θ_1'/h versus h^2 and Θ_1''/h versus h^2 at various T to (3) and its equivalent equation

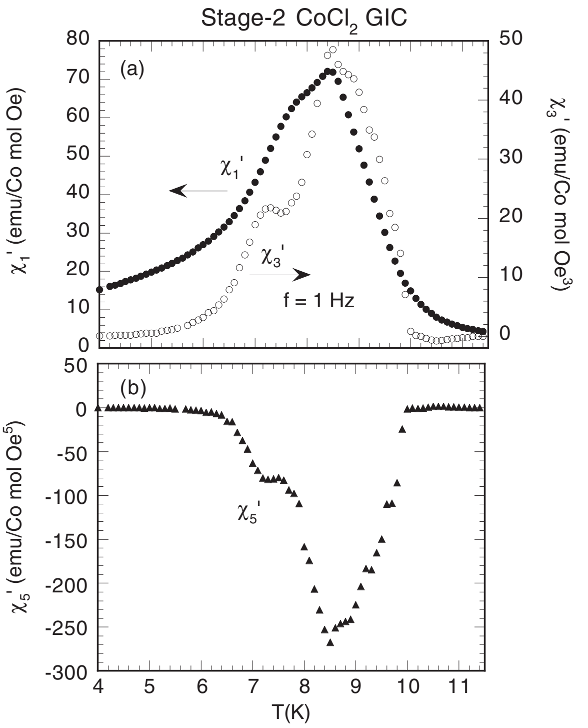

Figure 7. T dependence of (a) χ_1' (●) and χ_3' (○) and (b) χ_5' (▲), where the units of χ_{2n+1}' are emu/(Co mol Oe^{2n+1}).

with power forms up to h^4 yields the nonlinear susceptibilities χ_{2n+1}' and χ_{2n+1}'' ($n = 0, 1, 2$). Note that only the data for $0.15 \leqslant h \leqslant 0.5$ Oe are used for the analysis because in a strict sense the expansion given by (3) is valid only in the vicinity of $h = 0$.

Figures 7(a) and (b) show the T dependences of χ_1', χ_3' and χ_5'. The nonlinear susceptibility χ_3' shows positive peaks at T_{cl} and T_p and a positive shoulder at T_{cu}, while χ_5' shows negative local minima around T_{cl} and T_p and a negative shoulder around T_{cu}. The detail of the T dependence of χ_3' and χ_5' above 10 K is described as follows. The susceptibility χ_3' is zero around 11.2 K, decreases with decreasing T and exhibits a negative local minimum at 10.5 K. In turn it increases with further decreasing T and becomes positive below 10.2 K. In contrast, χ_5' is zero at 11.2 K, increases with decreasing T and exhibits a positive local maximum at 10.5 K. In turn it decreases with further decreasing T and becomes negative below 10.3 K. Figures 8(a) and (b) show the T dependence of χ_1'', χ_3'' and χ_5''. The susceptibility χ_3'' has positive peaks at T_{cl}, T_p and T_{cu}, while χ_5'' has negative local minima at T_{cl}, T_p and T_{cu}. The sign of χ_3'' changes from negative to positive around 10.8 K with decreasing T. The sign of χ_5'' changes from negative to positive around 10.8 K, and from positive to negative between 5.9 and 6.0 K with decreasing T.

Here we give some justification for the use of the field range ($0.15 \leqslant h \leqslant 0.5$ Oe) for the above least-squares fits. Using the values of χ_1', χ_3' and χ_5', experimentally obtained, we can calculate the critical fields $h_c^{(1)}$ ($=2|\chi_1'/\chi_3'|^{1/2}$) at which the first term of Θ_1'/h in (3) is comparable to the second term. The field $h_c^{(1)}$ is 5.9 Oe at 6 K and tends to decrease to 2.1 Oe at 9.5 K, and increases with further increasing T. Thus the expansion series given by (3) are valid for $0.15 \leqslant h \leqslant 0.5$ Oe since $h_c^{(1)}$ is much larger than 0.5 Oe.

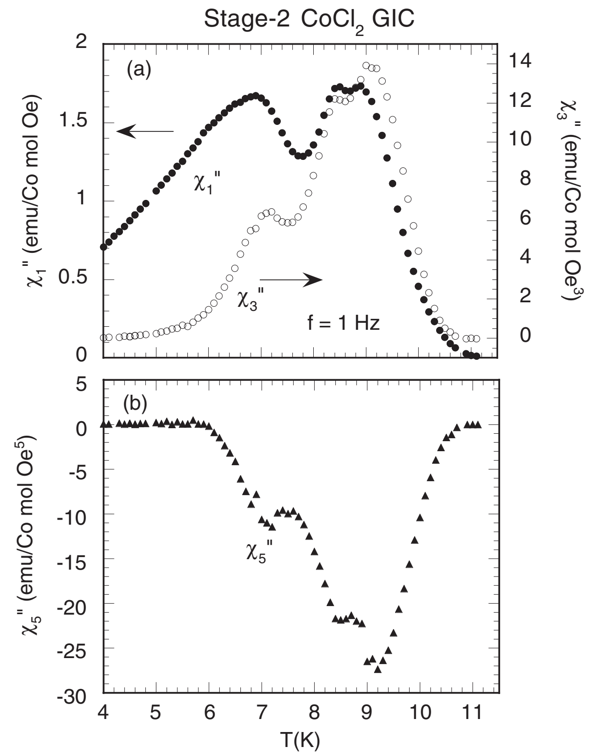

Figure 8. T dependence of (a) χ_1'' (●) and χ_3'' (○) and (b) χ_5'' (▲), where the units of χ_{2n+1}'' are emu/(Co mol Oe^{2n+1}).

5. Discussion

5.1. H–T phase diagram

We have determined the H–T diagram near T_{cu} and T_{cl}, which is shown in figure 9. Here the open and closed circles denote the peak temperatures of Θ_1'/h versus T and Θ_1''/h versus T shown in figures 2(a) and (b). Note that there is no open circle below T_{cl} in the (T, H) plane, indicating that the phase transition below T_{cl} can be observed by Θ_1''/h, but not by Θ_1'/h. For convenience we define the lines H_{c1}, H_{c2}, H_{c3} and H_+. The lines H_{c1} and H_{c2} intersect at a point ($T_1 = 7.5$ K, $H_1 = 43$ Oe), while the lines H_{c2} and H_+ intersect at a point ($T_2 = T_p = 8.4$ K, $H_2 = 161$ Oe). The line H_{c3}, which originates from $T = T_{cl}$ and $H = 0$, increases with decreasing T. A metamagnetic transition may occur on the line H_{c3}, because there is no line above H_{c3} below T_{cl}. If the extrapolation of the line H_{c3} to $T = 0$ K corresponds to H_E', H_E' is larger than $H_{c3} = 45$ Oe at $T = 6.3$ K. This is consistent with the value of H_E' (=93 Oe), which is estimated from the DC magnetic susceptibility χ along the c plane ($\chi = 96$ emu/Co mol Oe at $H = 10$ Oe and $T = 4.2$ K), where χ is related to H_E' by $\chi = N_A g_a \mu_B S/(2H_E')$. The line H_+ above T_{cu} is due to FM spin fluctuations which are noncritical. The line H_{c1}, which originates from $T = T_p$ and $H = 0$, increases with decreasing T. The magnitude of H_{c1} is of the same order as that reported by Nicholls and Dresselhaus [19]: $H_{c1} = 4$ Oe at $T = 4$ K. The H–T diagram above T_{cl} is much complicated than we expected. Since there is no AF spin correlation between spins in adjacent layers, the line H_{c1} does not correspond to the spin-flop transition line. The line H_{c1} may be related to the sixfold-symmetry-breaking field H_A^{in} (see section 5.4).

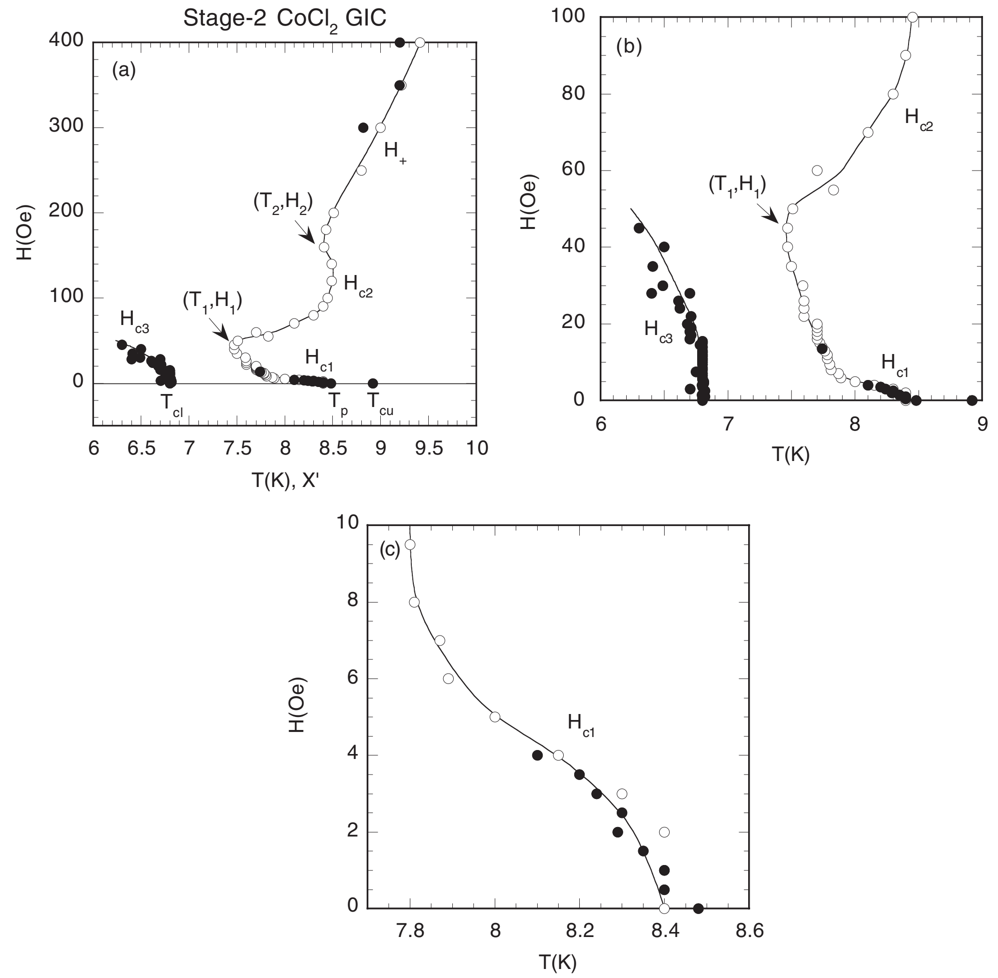

Figure 9. (a)–(c) H–T diagram which is determined from the peak temperatures of Θ_1'/h versus T (○) and Θ_1''/h versus T (●) in figure 2: $H \perp c$. The solid curves are guides to the eyes. The definitions of the lines H_{ci} ($i = 1$–3) and H_+ and two points (T_1, H_1) and (T_2, H_2) are given in the text.

5.2. *Nature of the low-temperature phase below* T_{cl}

The decrease of T_{cl} with decreasing f is a characteristic feature of spin-glass-like behaviour. Here we discuss the f dependence of the peak temperature (T_{cl}) of Θ_1''/h ($\approx \chi_1''$). In spite of possible distribution of relaxation times, we assume that χ_1'' has a peak at $\omega\tau = 1$, where ω ($=2\pi f$) is the angular frequency and τ is the average relaxation time of the system. Figure 10 shows the T dependence of τ. It divergingly increases with decreasing T. The relaxation time τ may be described by a power-law form

$$\tau = \tau_0^*(T/T^* - 1)^{-x}, \tag{5}$$

where $x = z\nu$, z is a dynamic critical exponent, ν is an exponent of the spin correlation length, T^* is a finite spin-freezing temperature and τ_0^* is a characteristic time. The least-squares fit of the data of τ versus T over the temperature range $6.8 \leqslant T \leqslant 7.2$ K to (5) yields the parameters $x = 7.55 \pm 1.87$, $T^* = 6.71 \pm 0.08$ K and $\tau_0^* = (2.06 \pm 0.05) \times 10^{-13}$ s. The value of T^* is

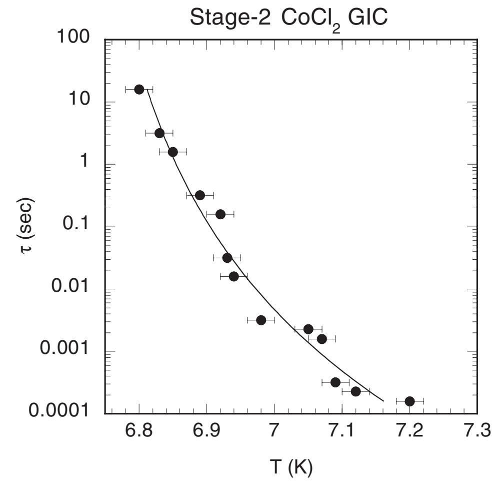

Figure 10. T dependence of τ which is determined from the f dependence of peak temperature T_{cl} in the data of χ_1'' versus T with various f in figure 1. The solid curve denotes the least-squares fit of the data to (5).

very close to T_{cl} at $f = 0.01$ Hz. Our result is compared with the experimental result obtained by Gunnarsson *et al* [20] for a typical three-dimensional Ising SG with short-range interaction, $Fe_{0.5}Mn_{0.5}TiO_3$: $x = 10.0 \pm 1.0$, $T^* = 20.95 \pm 0.10$ K and $\tau_0^* = 1.58 \times 10^{-13}$ s. The value of x for the stage-2 $CoCl_2$ GIC is smaller than that for $Fe_{0.5}Mn_{0.5}TiO_3$, but the values of τ_0^* are almost the same. We also note that our value of x is in good agreement with the theoretical prediction by Ogielski [21] from Monte Carlo simulation of a three-dimensional ($\pm J$) Ising spin-glass model with short-range interactions: $x = 7.9 \pm 1.0$.

Another possible source for the divergence of τ is thermally activated relaxation over energy barriers. The basic idea of activated dynamics is to define a droplet in the ground state as the lowest-energy excitation of length scale L [22]. The thermal activation over the energy barrier height B ($\approx L^{\psi}$) is assumed for the droplets which are thermally active, where ψ is an exponent. The relaxation time for the droplet with $L = \xi$ is given by a generalized Arrhenius law

$$\tau = \tau_0 \exp\left(\frac{B}{T}\right) \qquad \text{or} \qquad \ln\left(\frac{\tau}{\tau_0}\right) = \left(\frac{b}{T}\right)^{1+\psi\nu}, \tag{6}$$

where ξ is the spin correlation length, $\xi \approx T^{-\nu}$ for a zero-temperature critical point, ν is a critical exponent of ξ, τ_0 is the microscopic single-spin relaxation time and $B = b^{1+\psi\nu}/T^{\psi\nu}$. A simple Arrhenius law corresponds to the case of $\psi\nu = 0$. The least-squares fit of the data τ versus T to (6) yields $\tau_0 = (4.6 \pm 0.5) \times 10^{-6}$ s, $1 + \psi\nu = 27.5 \pm 6.7$ and $b = 7.5 \pm 1.0$ K for $6.8 \leqslant T \leqslant 7.2$ K. The data fit quite well to the resulting fitting curve. Nevertheless, such an unphysical value of $(1+\psi\nu)$ suggests that the droplet model is inappropriate for the present case.

Is there any evidence of the RSG-like behaviour in the magnetic neutron scattering in the stage-2 $CoCl_2$ GIC? Below T_{cl}, AF Bragg reflections appear at $L = 1/2, 3/2$ and $5/2$ along $(00L)$, where Q_c ($=Lc^*$) is the wavenumber, $c^* = 2\pi/d$ and d is the distance between the adjacent Co layers [23,24]. These AF peaks are much broader than instrumental resolution, and moreover have line shapes that are Lorentzian rather than Gaussian. These features indicate that the reflections are associated with short-range spin order rather than long-range spin order. The spin correlation length along the c axis drastically increases with decreasing T below T_{cl}, but saturates to a constant value of 22 Å, or less than two $CoCl_2$ layers. In addition to the

AF Bragg reflections, there is a broad background forming a magnetic ridge along the c^* axis. This ridge may reflect the two-dimensionality of spin–spin correlations. The ridge intensity starts to increase at T_{cu} and remains very intense at 4.4 K. There is no anomaly around T_{cl}.

It seems that there is no positive evidence of the RSG phase from the T dependence of AF Bragg intensities in the stage-2 $CoCl_2$ GIC. However, the high intensity of the magnetic ridge at low T may be related to the existence of the RSG phase. The magnetic ridge corresponds to the magnetic diffuse scattering around the AF Bragg reflections. This implies that the existence of the RSG phase may be detected by magnetic diffuse scattering around the AF Bragg reflections, but not by the AF Bragg intensity. In fact this conclusion is similar to those derived from the magnetic neutron scattering on three-dimensional Ising RSG systems $Fe_{0.6}Mn_{0.4}TiO_3$ [25] and $Fe_{0.55}Mg_{0.45}Cl_2$ [26], where the RSG phase below T_{RSG} is a mixed phase of the SG and AF phase. For $Fe_{0.6}Mn_{0.4}TiO_3$ [25], the AF Bragg reflection grows below T_N like an ordinary antiferromagnet and persists below T_{RSG} ($<T_N$), indicating that the AF order below T_N is unaffected by the RSG transition. The diffuse scattering near the AF Bragg reflection shows two peaks at T_N and T_{RSG}. The intensity remains very intense at lower temperatures below T_{RSG}. For $Fe_{0.55}Mg_{0.45}Cl_2$ [26], the AF order persists below T_{RSG}. The diffuse scattering shows only one peak at T_N because of a critical scattering. No anomaly is observed below T_N. The intensity is much higher than the background at low T.

5.3. χ_3' at T_{cl}

Takayama [8] has investigated magnetic responses of mean-field models for RSG phases by making use of the prescription described in section 2.1. The models examined are the original SK ($J_0 > J_1$) and its two extensions: the random-network FM-SG model [27] and the enhanced AF-SG model [28]. All these systems exhibit the RS–RSB transition at T_{RSG}, keeping spontaneous (staggered) magnetization finite. The magnetic response has the following features.

(i) Both χ_1 and χ_3 exhibit positive cusps at T_{RSG}.
(ii) Both χ_1 and χ_3 decrease quite significantly with decreasing T below T_{RSG}.
(iii) The relaxation time τ diverges at T_{RSG}.

For comparison, we assume that the above theories for χ_1 and χ_3 are also true for χ_1' and χ_3'. Experimentally, χ_1' has an inflection point just above T_{cl}, but χ_3' has a small positive peak around T_{cl} (see figure 7). These results are in good agreement with the above predictions, suggesting that the low-temperature phase below T_{cl} may be a mixture of SG phase and AF phase (RSG phase). Because of the complicated interactions in the stage-2 $CoCl_2$ GIC, it is difficult to define which class our system belongs to (FM-RSG or AM-RSG). However, this classification is not so important because a cusplike structure is predicted for both FM-RSG and AM-RSG.

In spite of such an agreement, there is some concern whether specific features seen in higher-order nonlinear susceptibility may not necessarily correspond to the RSG transition in thermal equilibrium. This problem is closely related to the non-ergodicity of the RSB phase. There exist many local minima of the free energy (pure states). Theoretically, there are two kinds of magnetic AC response in the RSB phase. One is the magnetic AC response in thermal equilibrium in which reconstruction of global energy structure by the application of AC field h is involved. The other is the magnetic AC response for one of the free-energy local minima (pure state) in the RSB phase where the system is trapped. The latter are fast responses in the nonequilibrium state as compared with the slow response in thermal equilibrium. Experimentally, the separation between fast and slow responses is by no means well established for realistic SG and RSG systems. We note that similar situations are also encountered in the DC magnetic susceptibility measurement. In the susceptibility χ_{FC}, a global response to H of the whole free-energy structure is involved. On the other hand, the susceptibility χ_{ZFC} is attributed to the response to H of one of the pure states where the system is trapped. In the stage-2 $CoCl_2$ GIC [3], χ_{ZFC} at $H = 1$ Oe shows a peak at 8.2 K, while $d\chi_{ZFC}/dT$ has a maximum at 6.6 K close to T_{cl}. This is similar to the case of a normal antiferromagnet, where T_N is not a peak temperature of the DC magnetic susceptibility χ, but a temperature at which $d\chi/dT$ has a maximum. In this sense, the T dependence of χ_{ZFC} gives some evidence for the RSG phase below T_{cl}, in spite of the behaviour measured in the nonequilibrium state.

The magnetic responses which Takayama [8] has calculated are fast responses, which are not always the same as the slow responses in thermal equilibrium. Therefore it may be reasonable to compare our data with the theoretical prediction, even if our data are not taken in thermal equilibrium. In order to examine the thermodynamic phase transition from the nonlinear susceptibility measurement, it is necessary to use equilibrium data in the T range where χ_1'' is too small to be detected. In our system, χ_1'' is present at all T below 10 K, implying that no data around T_{cu} and T_{cl} are taken in thermal equilibrium.

What kind of spin frustration effect occurs in the stage-2 $CoCl_2$ GIC, leading to the RSG-like behaviour? There are at least two kinds of competing interaction [1–3]. One is the intraplanar FM interaction J. The other is the effective AF interplanar interaction, J'_{eff}, which is of the order of $J'(\xi_a/a)^2$, where J' (<0) is the AF interplanar exchange interaction ($|J'|/J \approx 10^{-4}$), ξ_a is the in-plane spin correlation length and a (=3.55 Å) is the in-plane lattice constant [23]. The growth of ξ_a is partly limited by the existence of small islands. The size of ξ_a may increase in two steps, giving rise to the successive phase transitions at T_{cu} and T_{cl} [1, 2]. Since ξ_a increases but does not diverge on approaching T_{cl}, the magnitude of J'_{eff} remains comparable to that of FM intraplanar interaction J. The spin frustration effect occurs as a result of the competition between these two interactions, leading to the RSG behaviour.

5.4. χ_3' above T_{cu}

As far as we know, the studies for χ_3 for a regular ferromagnet and antiferromagnet are not so numerous as those for spin glasses. For a ferromagnet, Fujiki and Katsura [29] have developed a theory of χ_3 on the basis of the Bethe approximation. They have predicted that χ_3 diverges on both sides of T_c. The sign of χ_3 changes from negative to positive at T_c as T decreases. For an antiferromagnet, χ_3 undergoes a steplike change at T_N. The sign of χ_3 changes from negative to positive at T_N as T decreases. Kawamura [30] has predicted the T dependence of χ_3 from his Monte Carlo simulation in the case when the spin fluctuation effect is taken into account in the molecular field theory. He has shown that the T dependence of χ_3 near T_N for an antiferromagnet is rather different from the steplike change of χ_3 at T_N predicted by Fujiki and Katsura [29]. For the system with Ising symmetry, χ_3 is positive above T_N, increases with decreasing T and shows a peak just above T_N. For the system with Heisenberg or XY symmetry, χ_3 is negative above T_N, partly because the spin direction becomes perpendicular to the direction of the field.

Figure 11 shows the T dependence of the peak field h_p for $\Delta(\Theta_1'/h)$ versus h, the line H_{c1} and χ_3'. As pointed out in section 4.2.3, χ_3' exhibits a negative local minimum at 10.5 K and becomes positive below 10.2 K. Note that similar behaviour of χ_3' in $(C_2H_5NH_3)_2CuCl_4$ is observed above T_N (=10.33 K) [31]. Below T_N, there exists the three-dimensional AF phase where the two-dimensional FM layers are antiferromagnetically stacked along the c axis. The peak field h_p starts to increase below 10.3 K with decreasing T and almost coincides

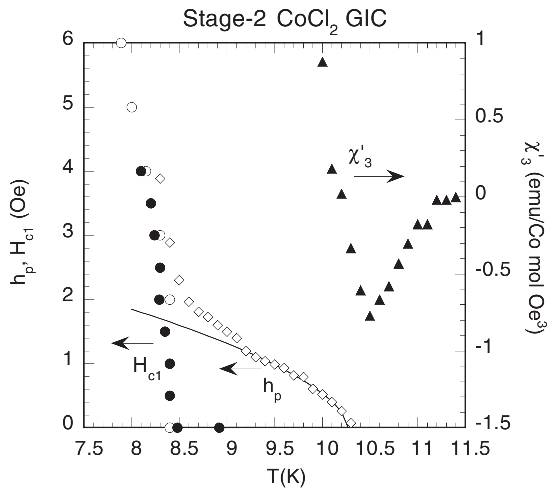

Figure 11. T dependence of the peak field h_p (◇) for $\Delta(\Theta_1'/h)$ versus h, the line H_{c1} determined from the peak temperatures of Θ_1'/h versus T (○) and Θ_1''/h versus T (●) in figure 2, and χ_3' (▲). The solid curve for h_p denotes a least-squares fitting curve. See the text for details.

with the line H_{c1} below T_p. The T dependence of h_p is experimentally described by a relation $h_p = h_p^0(1-T/T_g)^\mu$ for $9.2 \leqslant T \leqslant 10.3$ K, where $h_p^0 = 4.46\pm0.60$ Oe, $T_g = 10.28\pm0.03$ K and an exponent $\mu = 0.58\pm0.06$. The value of h_p^0 is of the same order as that of H_A^{in} (=10 Oe) reported by Karimov [32], suggesting that h_p is a measure for the Ising symmetry arising from the field H_A^{in}.

In spite of the fact that the discussion is restricted to the T dependence of χ_3 above T_N for an antiferromagnet in Kawamura's theory [30], we assume that this theory is applicable to the critical behaviour of χ_3' above T_{cu} in the stage-2 $CoCl_2$ GIC where the FM short-range order is dominant. Then the T dependence of χ_3' above T_{cu} for the stage-2 $CoCl_2$ GIC may be explained as follows. The negative local maximum of χ_3' at 10.5 K and the zero crossing at 10.2 K may correspond to the crossover of the symmetry in spin fluctuations from two-dimensional Heisenberg to two-dimensional XY and from two-dimensional XY to two-dimensional Ising, respectively. The XY and Ising character of the system are due to the easy-plane type anisotropy field H_A^{out} and the in-plane anisotropy field H_A^{in}, respectively. Because of H_A^{in}, the spins tend to align along the easy axis with sixfold symmetry in the c plane.

5.5. *T dependence of* Θ_3'/h^3

We compare our result on the T dependence of χ_3' for the stage-2 $CoCl_2$ GIC with those reported by Matsuura and Hagiwara [5]. They have measured the third-harmonic in-phase component of AC magnetization as a nonlinear magnetic response to an AC magnetic field. As given in (4), Θ_3'/h^3 coincides with $\chi_3'/4$ for small h, but it includes higher-order terms such as $5\chi_5'h^2/16$ and $21\chi_7'h^4/64$ for large h. Matsuura and Hagiwara [5] have shown that Θ_3'/h^3 at $h = 0.2$ Oe ($f = 0.1$ Hz) exhibits a negative local minimum around 9.5 K. The sign of Θ_3'/h^3 changes from negative to positive around 9 K with decreasing T. The susceptibility Θ_3'/h^3 has a positive shoulder at 8.3 K and a positive broad peak at 7.1 K. Their result is similar to our result of χ_3' shown in figure 7(a), in spite of the slight difference in temperature. In contrast, Θ_3'/h^3 at $h = 0.8$ Oe ($f = 0.1$ Hz) exhibits a negative local minimum at 8.9 K and a positive peak at 6.6 K. The sign of Θ_3'/h^3 changes from negative to positive at 7.2 K with decreasing T. Their result at $h = 0.8$ Oe is rather different from that at $h = 0.2$ Oe ($f = 0.1$ Hz), indicating that the contribution from the higher-order term $5\chi_5' h^2/16$ to Θ_3'/h^3 becomes significant even at $h = 0.8$ Oe. Using our values of χ_3', and experimentally obtained χ_5', we can in fact estimate the critical field $h_c^{(3)}$ $(=|4\chi_3'/5\chi_5'|^{1/2})$ at which the first term of Θ_3'/h^3 in (4) is comparable to the second term: $h_c^{(3)} = 0.9$ Oe at 6 K. This implies that Θ_3'/h^3 is approximated by $\chi_3'/4$ only for $h \ll h_c^{(3)}$. In order to see how the T dependence of Θ_3'/h^3 is influenced by the second term $5\chi_5' h^2/16$, we calculate Θ_3'/h^3 using (4) with χ_3' and χ_5' determined by our method. The T dependence of Θ_3'/h^3 thus calculated for $h = 0.5$ Oe has the following feature. The positive peak around 8–9 K for $h < 0.35$ Oe is due to χ_3' and the negative peak for $h > 0.4$ Oe is due to χ_5'. We find that the T dependence of Θ_3'/h^3 at $h = 0.8$ Oe ($f = 0.1$ Hz) by Matsuura and Hagiwara [5] is very similar to that calculated at $h = 0.5$ Oe. This result suggests that the contribution of χ_5' is comparable to or even larger than that of χ_3' for $h > 0.4$ Oe. Since χ_3' is not exactly derived in the measurement made by Matsuura and Hagiwara [5], their interpretation of the data is inappropriate.

6. Conclusion

We have studied the linear and nonlinear AC magnetic susceptibility of the stage-2 $CoCl_2$ GIC. The temperature and frequency dependence of the linear AC magnetic susceptibility (χ_1' and χ_1'') indicates that this compound undergoes magnetic phase transitions at T_{cu} and T_{cl}. The peak of χ_1'' at T_{cl} shifts to the low-T side with decreasing f. The nonlinear susceptibility χ_3' shows a positive peak around T_{cl}. These results suggest the possibility of the re-entrant spin-glass phase where the AF and SG phases coexist. Magnetic diffuse scattering experiments will be required to further the understanding of the nature of the RSG phase below T_{cl}. The change of sign in χ_3' from negative to positive above T_{cu} with decreasing T is indicative of the growth of two-dimensional FM spin order inside $CoCl_2$ layers. The crossover behaviour of the critical behaviour from XY symmetry to Ising symmetry is clearly seen in the T dependence of χ_3' and the peak field of $\Delta(\Theta_1'/h)$ versus h.

Acknowledgments

We thank Professor H Kawamura for his valuable comment and Professor A Ito for showing us results of nonlinear AC magnetic susceptibility of $Fe_cMn_{1-c}TiO_3$ before publication. We are grateful to Professor H Suematsu for providing the us with single crystals of kish graphite. This work was supported by SUNY-Binghamton Research Foundation (contract number 240-9522A).

References

[1] Dresselhaus G, Nicholls J T and Dresselhaus M S 1990 *Graphite Intercalation Compounds* vol 2, ed H Zabel and S A Solin (Berlin: Springer) p 247 and references therein
[2] Suzuki M 1990 *Crit. Rev. Solid State Mater. Sci.* **16** 237 and references therein
[3] Suzuki M and Suzuki I S 1998 *Phys. Rev.* B **58** 840
[4] Binder K and Young A P 1986 *Rev. Mod. Phys.* **58** 801
[5] Matsuura M and Hagiwara M 1990 *J. Phys. Soc. Japan* **59** 3819
[6] Miyoshi K, Hagiwara M and Matsuura M 1996 *J. Phys. Soc. Japan* **65** 3306
[7] Suzuki M 1977 *Prog. Theor. Phys.* **58** 1151
[8] Takayama H 1996 *J. Phys. Soc. Japan* **65** 1450
[9] Kunkel H P and Williams G 1988 *J. Magn. Magn. Mater.* **75** 98

[10] Chakravarti A, Ranganathan R and Chatterjee S 1994 *J. Magn. Magn. Mater.* **138** 329
[11] Ando T, Yanagihara H, Sato T and Ohta E 1995 *J. Magn. Magn. Mater.* **140–144** 1783
[12] Tobo A and Ito A 1998 *J. Phys. Soc. Japan* **67** 297
[13] Fujii K 1996 *Master Thesis* Ochanomozu University Department of Physics
[14] Mézard M, Parisi G and Virasoro M A 1987 *Spin Glass Theory and Beyond* (Singapore: World Scientific)
[15] Sherrington D and Kirkpatrick S 1975 *Phys. Rev. Lett.* **35** 1792
[16] Wiesler D G, Suzuki M, Chow P C and Zabel H 1986 *Phys. Rev.* B **34** 7951
[17] Levy L P and Ogielski A T 1986 *Phys. Rev. Lett.* **57** 3288
[18] Mydosh J A 1993 *Spin Glasses: an Experimental Introduction* (London: Taylor and Francis)
[19] Nicholls J T and Dresselhaus G 1990 *J. Phys.: Condens. Matter* **2** 8391
[20] Gunnarsson K, Svedlindh P, Nordblad P, Lundgren L, Aruga H and Ito A 1988 *Phys. Rev. Lett.* **61** 754
[21] Ogielski A T 1985 *Phys. Rev.* B **32** 7384
Ogielski A T 1987 *Heidelberg Colloquium on Glassy Dynamics (Lecture Notes in Physics)* vol 275, ed J L van Hemmen and I Morgenstern (Berlin: Springer) p 190
[22] Fisher D S and Huse D A 1988 *Phys. Rev.* B **38** 386
[23] Wiesler D G, Suzuki M and Zabel H 1987 *Phys. Rev.* B **36** 7051
[24] Wiesler D G, Zabel H and Shapiro S M 1994 *Z. Phys.* B **93** 277
[25] Yoshizawa H, Mitsuda S, Aruga H and Ito A 1987 *Phys. Rev. Lett.* **59** 2364
[26] Wong P-Z, von Molnar S, Palstra T T M, Mydosh J A, Yoshizawa H, Shapiro S M and Ito A 1985 *Phys. Rev. Lett.* **55** 2043
[27] Takayama H 1992 *J. Phys. Soc. Japan* **61** 2512
[28] Takayama H 1988 *Prog. Theor. Phys.* **80** 827
[29] Fujiki S and Katsura S 1981 *Prog. Theor. Phys.* **65** 1130
[30] Kawamura H 2000 private communication
[31] Narita N and Yamada I 1996 *J. Phys. Soc. Japan* **65** 4054
[32] Karimov Yu S 1974 *Sov. Phys.–JETP* **39** 547